Journal of Flow Control, Measurement & Visualization, 2022, 10, 32-55
https://www.scirp.org/journal/jfcmv
ISSN Online: 2329-3330
ISSN Print: 2329-3322

Three-Dimensional Velocity Distribution Measurement Using Ultrasonic Velocity Profiler with Developed Transducer

Naruki Shoji[1], Hiroshige Kikura[1], Hideharu Takahashi[1], Wongsakorn Wongsaroj[2]

[1]Laboratory for Zero-Carbon Energy, Tokyo Institute of Technology, Tokyo, Japan
[2]Department of Instrumentation and Electronics Engineering, King Mongkut's University of Technology North Bangkok, Bangkok, Thailand
Email: shoji@us.nr.titech.ac.jp

How to cite this paper: Shoji, N., Kikura, H., Takahashi, H. and Wongsaroj, W. (2022) Three-Dimensional Velocity Distribution Measurement Using Ultrasonic Velocity Profiler with Developed Transducer. *Journal of Flow Control, Measurement & Visualization*, **10**, 32-55.
https://doi.org/10.4236/jfcmv.2022.101003

Received: September 3, 2021
Accepted: October 22, 2021
Published: January 14, 2022

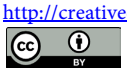

Abstract

This study describes an ultrasonic velocity profiler that uses a new ultrasonic array transducer with unique 5-element configuration, with all five elements acting as transmitters and four elements as receivers. The receivers are designed to reduce the amount of uncertainty. As the fluid moves through this setup, four Doppler frequencies are obtained. The multi-dimensional velocity information along the measurement line can be reconstructed. The transducer has a compact geometry suitable for a wide range of applications, including narrow flow areas. The transducer's basic frequency and sound pressure are selected and evaluated to be compatible with the application. First, to confirm the measurement ability, the measurement of the developed system in two-dimensional flow is validated by comparing it to the theoretical data. The uncertainty of measurement was within 15%. Second, the three-dimensional measurement in turbulent and swirling flow is proved experimentally to check the applicability of the proposed technique.

Keywords

Doppler Frequency, Liquid Velocity, Three-Dimensional Measurement, Transducer Design, Ultrasonic

1. Introduction

The visualization of flow field or velocity distribution is a critical task in fluid engineering. For engineering design, experimental investigation, or in-field maintenance, this is critical. The appearance of the flow field in multi-dimensional form occurs in numerous scenarios and must be visualized. In the pressurized water

reactor (PWRs), the coolant flow in multi-dimensional motion has been applied in nuclear fuel assemblies to enhance heat transfer in the reactor core. The grid spacer was used as a swirling generator and installed in rod bundles [1]. Furthermore, whirling flow, which has a multi-dimensional motion, is used in pneumatic conveying technology to reduce pressure drop and prevent particle deposition and clogging in the pipeline [2]. In the industrial process, cyclone separators have been used to purify a fluid stream of solid particles. The mechanism for separating the particles is the strong centrifugal force acting on the particle in the cyclone's swirling flow [3].

The multi-dimensional flow field, as defined above, can be found in a variety of process technologies. It is directly related to improving the efficiency of an industrial operation. It is necessary to do experimental research in order to comprehend the mechanism of the multi-dimensional flow distribution. As a result, a measurement approach is required to complete this inquiry.

Probe techniques have been used in velocity investigations, such as hot-wire [4], hot-film [5], etc. However, the measurement disturbs the flow field. The Laser Doppler Velocimetry (LDV) [6], a non-intrusive measurement, has been used to investigate the flow velocity in many applications. Nevertheless, probe techniques and LDV are one-point measurements and have a disability for multi-dimensional measurement. Kumar *et al.* [7] used particle tracking velocimetry (PTV) to visualize the secondary and primary flow in a cylindrical cyclone. Three-dimensional (3D) flow velocity distribution of swirling flow was observed. McClusky *et al.* [8] visualized swirling flow in a rod bundle sub-channel using particle image velocimetry (PIV). It was an effective experimental method to obtain the instantaneous velocity field and flow mapping.

However, in order to access the optical source and measure the flow field, these approaches necessitate the test section being transparent. Furthermore, due to the optical obstruction, these measuring techniques have difficulties applying if the channel or flow path under consideration is complex geometry or narrow flow path.

Ultrasonic Velocity Profiler (UVP) is a non-invasive measurement that does not require optical access and can work among opaque fluid. It has a broad range of applications. The UVP was proposed first in the medical application. Satomura [9] and Baker [10] used the UVP for blood flow measurement in one-dimensional.

Nonetheless, due to complex flow, which contains multi-dimensional motion, many therapeutic interest areas are unable to use this assumption. Peronneau *et al.* [11] proposed a single element cross beam system that uses two transducers as a transceiver that works transmitter and receiver respectively to measure two-dimensional velocity (2D) at the cross-point. This system can only obtain 2D velocity at one point, and requires mechanical adjustment to gather velocity data at other points. Scabia *et al.* [12] developed multiple elements cross beam system that uses two receivers to measure at one point and numerous receivers to gather velocity data from other points to derive the 2D velocity

profile. This system is large and can obtain only 2D velocity. Using three transducers as indicated in Fox's work [13], a comparable measurement system was further developed for measurement in the 3D flow field. However, this system is time-consuming since the transducers have to be operated separately to avoid the interference of the sound beam. Then, Dunmire *et al.* [14] developed a 3D measurement system using five transducers with only one transmitter and four receivers. The measurement occurs at the same time and same measurement volume. However, this measurement system was huge and had a limited application that is unable to apply in the complex geometry or narrow flow path.

Takeda [15] was the first to propose the UVP for measuring one-dimensional velocity profiles in the liquid in fluid engineering. It has been used to obtain velocity profiles in several liquids such as water [16], liquid metal [17], magnetic liquid [18], and liquid sodium [19]. In addition, liquid flowrate measuring [20] [21] has been used as an application. These UVP investigations, however, are a one-dimensional measurement. Then, Batsaikhan *et al.* [22] developed multiple elements cross beam system using a couple of 128-element sectorial array transducers, and velocity data are obtained at beam cross points. Hamdani *et al.* [23] constructed a two-dimensional and two velocity components measurement system using an 8-element phased array transducer and applied it to the piping flow in elbow layout [24] [25]. These measurement systems are only 2D measurements. Hurther and Lemmin [26] developed 3D velocity measurement in open-channel flow using one transmitter and four receivers. This measurement concept was practical to obtain the 3D velocity profile. Nevertheless, the transducer system was also large and not practical for a broad range of applications, especially in areas with limited space and geometry. To overcome this limitation, the transducer must be made to be compact practically and collaborate with the UVP system to obtain the multi-dimensional flow velocity distribution or flow filed in a wide application and supports the application in a small area.

This paper proposes a UVP measurement system with a five-element array transducer to measure multi-dimensional velocity profiles, whether two-dimensional or three-dimensional. These UVP investigations, on the other hand, are a one-dimensional measurement. One element works as a transmitter, and the four elements are transceivers. The active diameter of a transmitter is 5 mm. The transceiver is designed to minimize uncertainty. Four transceivers obtain four Doppler frequencies. The 2D or 3D velocity information along the measurement line can be reconstructed. The basic frequency and sound pressure of the transducer are analyzed. For confirming the measurement ability, firstly, the measurement of the developed system in 2D flow is validated by the theoretical data. Secondly, the 3D velocity profile measurement in turbulent and swirling flow is demonstrated experimentally.

2. Principle of Ultrasonic Velocity Profiler

The Ultrasonic Velocity Profiler (UVP) is a non-intrusive measurement for ob-

taining high time-spatial velocity profiles of liquids. The method does not require optical access, which can work on a non-transparent fluid. It is based on ultrasonic echography. Figure 1 shows the UVP principle, consisting of ultrasound transmission, echo signal, and velocity profile reconstructed. An ultrasonic pulse is emitted repeatedly, which accords to a pulse repetition frequency (f_{PRF}) from the transducer along the measurement line. The same transducer then receives the echo reflected from the reflector's surface, such as a small particle. A position of a particle can be calculated from the sound velocity c and traveling time of ultrasound τ from the start of the pulse burst to its reception.

$$i = \frac{c\tau}{2}. \tag{1}$$

Several echo sequences are needed. Doppler signal influenced by the velocity of a moving particle can be demodulated from the echo signals, as shown in Figure 2. The Doppler frequency $f_D(i)$ directly relates to the particle's velocity dispersed in the liquid (i is position). Hence, the velocity of the particle at that position $V(i)$ can be computed as

$$V(i) = \frac{cf_D(i)}{2f_0 \sin\theta}, \tag{2}$$

where f_0 is the basic frequency and θ is the incident angle. If the stokes number on the relation between small particles and liquid < 0.1, the particle will closely follow the liquid streamline. Then, several particles disperse in the liquid. Consequently, the velocity profile of the liquid can be obtained. In the UVP system, the Doppler pulse repetition, an accurate method, is used to extract the Doppler signal from the echo signals, estimate the Doppler frequency, and calculate liquid velocity, respectively. The Doppler signal is demodulated in the quadrature demodulation section. The echo signal $e(t)$ is reflected from the particle and obtained by the same transducer is expressed as

$$e(t) = A_{n,i} \cos 2\pi\left(f_0\left(t - t_{n,i}\right) + n\frac{f_{D,i}}{f_{PRF}}\right), \tag{3}$$

where n is pulse repetition, t_n represents the delay time of the echo at nth pulse repetition, and A is the amplitude.

In the quadrature demodulation section, the echo signals are multiplied by the cosine and sine function, and a finite impulse response filter is used as a low-pass filter to eliminate the basic frequency component. Therefore, the Doppler signal $DS_i(t)$ can be extracted from the echo signals as modeled in Equations (4) and (5).

$$\begin{aligned} DS_i(t) &= \left\{2e(t)\cos\left(2\pi f_0 t\right) + j\sin\left(2\pi f_0 t\right)\right\}_{LOWPASS}, \\ DS_i(t) &= \sum A_{n,i}\cos 2\pi\left(\frac{f_{D,i}n}{f_{PRF}} - f_0 t_{n,i}\right) - j\sum A_{n,i}\sin 2\pi\left(\frac{f_{D,i}n}{f_{PRF}} - f_0 t_{n,i}\right), \end{aligned} \tag{4}$$

$$DS_i(n) = A_{n,i}\cos\left(\frac{2\pi n f_{D,i}}{f_{PRF}} - \phi_i\right) - jA_{n,i}\sin\left(\frac{2\pi n f_D}{f_{PRF}} - \phi_i\right), \tag{5}$$

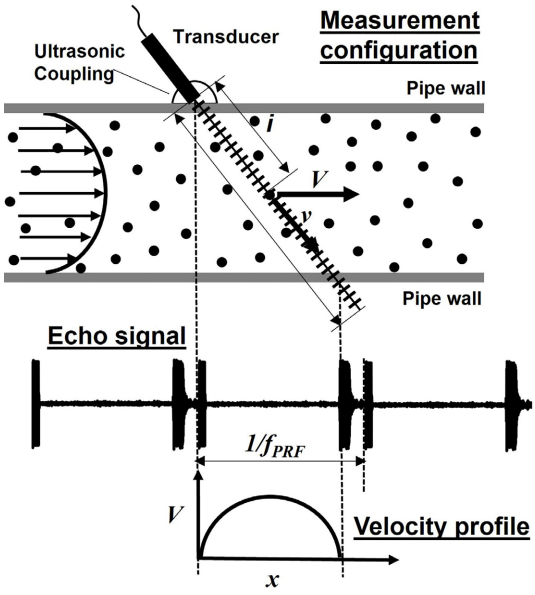

Figure 1. The ultrasonic velocity profiler principle.

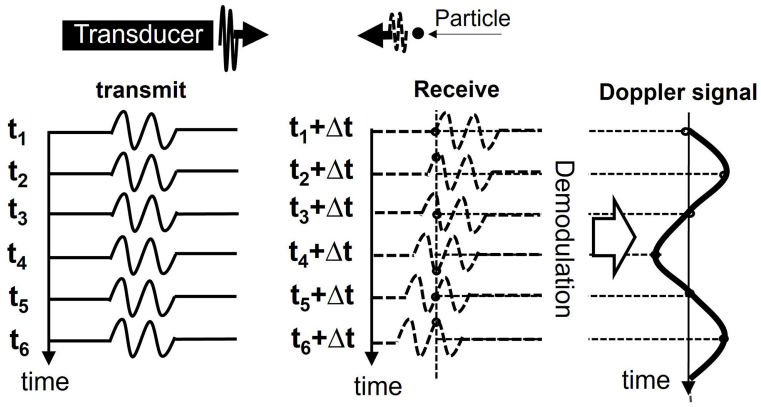

Figure 2. Doppler signal demodulation.

where φ is the initial phase, the Doppler frequency is then estimated in the frequency estimation section by a frequency estimator such as autocorrelation [27]. For autocorrelation, the method demonstrates a signal analysis to calculate the frequency of the Doppler signal. The autocorrelation function (R_m) derived from the Doppler signal $DS(n)$ of Equation (5) is expressed as follows:

$$R_m = \sum_{n=0}^{N_{rep}-2} DS[n] \times DS^*[n+1], \tag{6}$$

$$R_m = R_A + iR_B, \tag{7}$$

$$\begin{aligned} R_m = & \sum_{n=0}^{N_{rep}-2} \left(h_I[n] h_I[n+1] + h_Q[n] h_Q[n+1] \right) \\ & + i \sum_{n=0}^{N_{rep}-2} \left(h_I[n] h_Q[n+1] - h_I[n] h_Q[n+1] \right), \end{aligned} \tag{8}$$

where the * mark represents the complex conjugate, R_A and R_B are real and im-

aginary components of the autocorrelation function, and h_I and h_Q are in-phase and quadrature-phase components of the demodulated echo signal, respectively. The Doppler frequency can then be defined in Equation (9) as:

$$f_D = \frac{f_{PRF}}{2\pi} \tan^{-1} \frac{R_B}{R_A}. \tag{9}$$

Finally, the Doppler frequency estimated is plugged into Equation (2) to calculate the fluid velocity.

3. New Transducer Design and UVP System for Three-Dimensional Velocity Profile Measurement

3.1. Five-Element Transducer

To determine the ultrasonic basic frequency of a transducer, a simulation of sound intensity distribution was performed by using a distributed point source method (DPSM) [28], which is well known sound field calculation method. **Figure 3** shows the simulation result of the sound intensity distribution in each basic frequency; 2 MHz, 4 MHz, and 8 MHz. The single element transducer concept with an active diameter of 5 mm was used as a configuration for the simulation. The intensity, directivity, and near-field range are showed, respectively. The directivity was defined as the beam width where the beam intensity decreases to −6 dB in the main lobe region. The basic frequency at 2 and 4 MHz was revealed to attain a good intensity and directivity while having an acceptable near field length. The basic frequency at 4 MHz is a smaller wavelength than 2 MHz; it has a good sense for small particles. Therefore, the basic frequency of 4 MHz is chosen for this study.

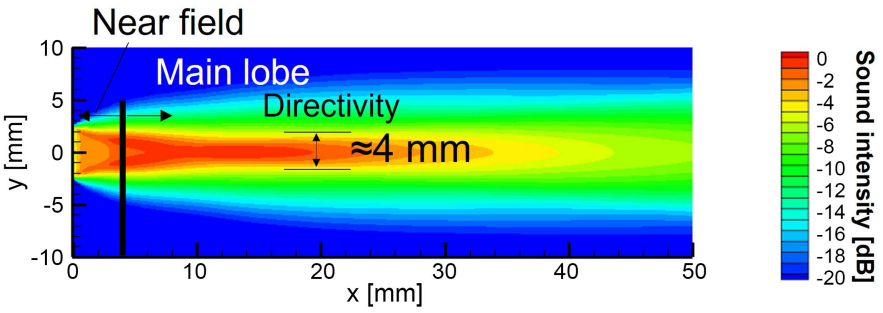

(a) 2 MHz

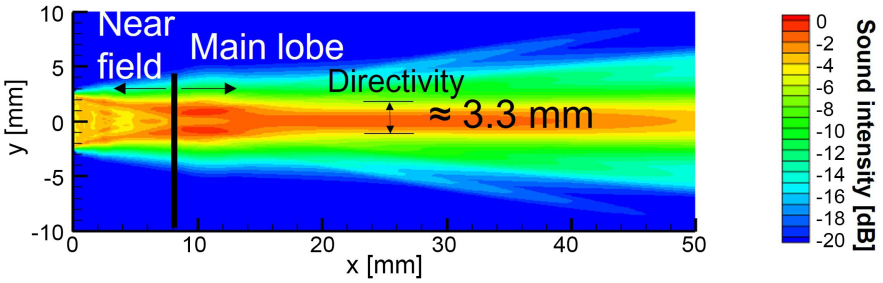

(b) 4 MHz

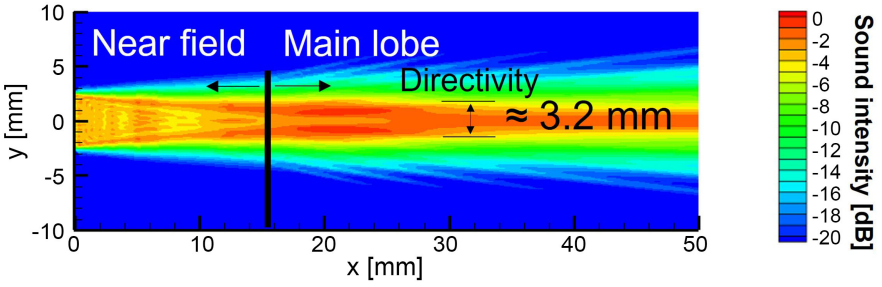

(c) 8 MHz

Figure 3. Simulation data of sound intensity distribution in each basic frequency.

Figure 4 shows a five-element transducer whose configuration was determined by the specifications in **Table 1**. The five-element transducer consists of a transmitter and four receivers. The transmitters send out an ultrasonic pulse, while the receivers receive echo signals simultaneously. The measurement principle is illustrated in **Figure 5**. The transducer was manufactured, as shown in **Figure 6**. As this configuration, the transducer can obtain four Doppler signals extracted from the echo derived in the measurement volume (channel) in each element with a certain echo angle (θ), as illustrated in **Figure 7**. The echo angle depends on channel distance and receiver position. Then, Doppler frequencies in each measurement channel ($f_D(i)$) are demodulated, respectively. For the receiver, the echo is required to reach the middle of the receiver element to minimize uncertainty. Hence, the element size (b) is specifically designed to be very small (approximately equal to wavelength ≈ 0.3 mm). Besides, the transmitter-receiver gap directly affects the transducer size. Therefore, it should be set to be as small as possible, where 0.1 mm is the smallest gap that the manufacturer can make it. The UVP system that integrates with the five-element transducer is shown in **Figure 8**. Using the four Doppler frequencies from one measurement volume, the 3D velocity profile, *i.e.*, axial velocity ($V_x(i)$), tangential velocity ($V_y(i)$) with the information of f_{D1} and f_{D2}, and radial velocity ($V_z(i)$) with the information of f_{D3} and f_{D4} can be obtained as Equations (10), (11) and (12). Then, the velocity profile in axial plane view (V_x-V_y) and radial plane view (V_z-V_y) can be reconstructed as shown in **Figure 9** with the Equations (13) and (14). Lastly, the 3D velocity profile or vector profile can be derived with Equation (15).

$$V_x(i) = \frac{c}{2f_0}\frac{f_{D1}(i) - f_{D2}(i)}{\sin\theta(i)} \tag{10}$$

$$V_y(i) = \frac{c}{2f_0}\frac{f_{D1}(i) + f_{D2}(i)}{1+\cos\theta(i)} \tag{11}$$

$$V_z(i) = \frac{c}{2f_0}\frac{f_{D3}(i) - f_{D4}(i)}{\sin\theta(i)} \tag{12}$$

$$V_{axial}(i) = \sqrt{V_x^2(i) + V_y^2(i)} \tag{13}$$

$$V_{radial}(i)=\sqrt{V_z^2(i)+V_y^2(i)} \tag{14}$$

$$V(i)=\sqrt{V_x^2(i)+V_y^2(i)+V_z^2(i)} \tag{15}$$

Table 1. Design of new transducer for 3D velocity measurement.

Specification	Detail
Basic frquency (f_0)	4 MHz
Wavelength in water, 20˚C (λ)	0.37 mm
Transmitter element width (a)	5 mm
Receiver element width (b)	0.3 mm
Transmitter-receiver gap (g)	0.1 mm
Element length (l)	5 mm

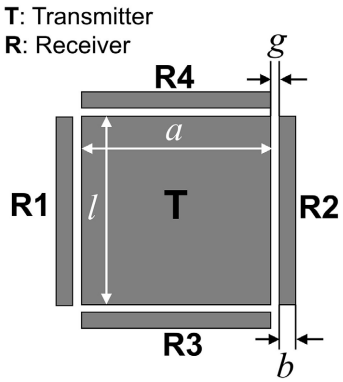

Figure 4. Ultrasonic element configuration on the five-element transducer (see **Table 1** for each dimension).

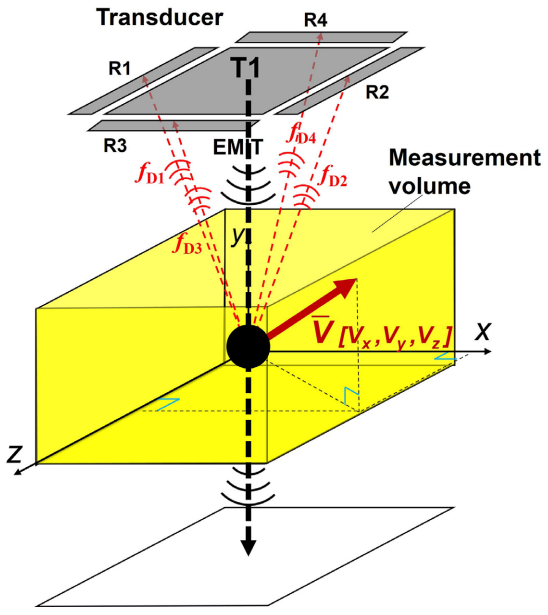

Figure 5. The measurement principle of the five-element transducer.

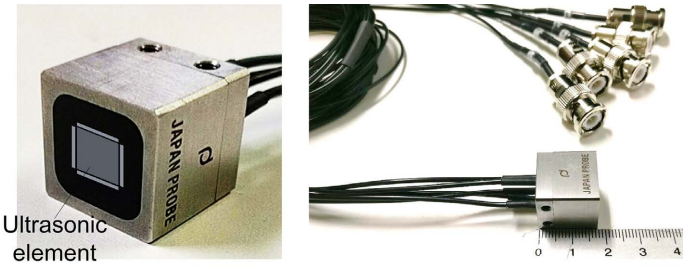

Figure 6. Image of the manufactured transducer.

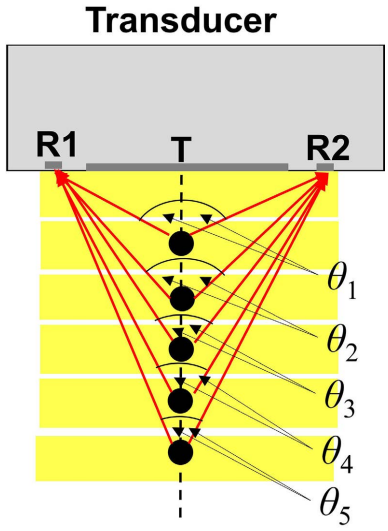

Figure 7. Illustration of echo angle.

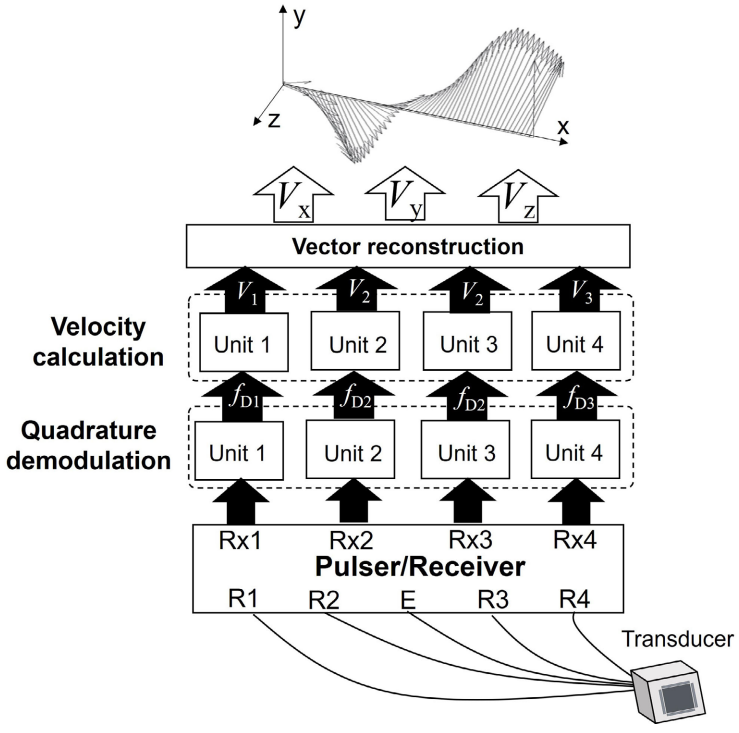

Figure 8. Measurement system of multi-dimensional measurement system.

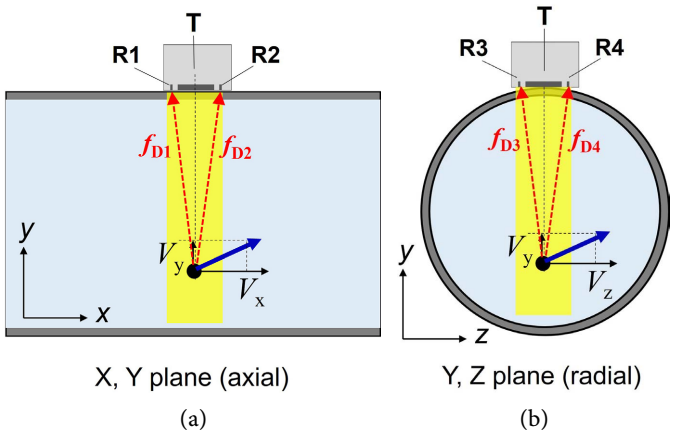

Figure 9. Schematic of measurement in an axial and a radial plane.

3.2. Sound Intensity Measurement

To test the sound field distribution of the manufactured transducer, sound intensity measurements were taken in a water tank. The ultrasonic pulse was transmitted from the center transmitter of a five-element transducer, while the needle hydrophone served as a receiver to extract the transmitted pulse. The measurement of a sound intensity distribution was in two-dimensional, and the sound intensity was assumed to be symmetric around the ultrasonic beam axis. The experimental setup is shown in Figure 10. An 8-channel pulser/receiver was used to operate the transducer (Model: JPR-10C-8CH3R, Japan Probe, Japan). The needle hydrophone was mounted on the XYZ stage controller, coupled to the A/D converter (National Instruments, USA, Model: NI PXI-5105 60 Ms/s), and the digital data were transferred to the computer (Model: Vostro, Dell, USA). The measurement processing was operated via LabVIEW software version 2011, respectively. The needle hydrophone moves automatically and the sound pressure measurement can be operated in a particular grid and positions in two-dimensional by automatically controlling the stage controller. In the experiment, the water temperature was controlled at 20˚C, the axial distance x was 50 mm, the half lateral distance y was 10 mm, and the axial resolution Δx and lateral resolution Δy was defined as 1 mm, respectively. The needle hydrophone was used to record the ultrasonic intensity (I) transmitted from the transducer, a peak-to-peak voltage. Then, the measurement data were analyzed and plotted on a color graph after being converted into sound intensity (SI) using the equation below.

$$SI = 20\log_{10}\frac{I}{I_{\max}}. \tag{16}$$

Figure 11 shows the sound intensity measurement result. In a five-element transducer, transmitting the ultrasonic wave by three elements simultaneously, there was the interference of sound waves from three elements, resulting in one main lobe sound field. The sound intensity obtained from the five-element transducer was compared with the single disk-like shape element transducer

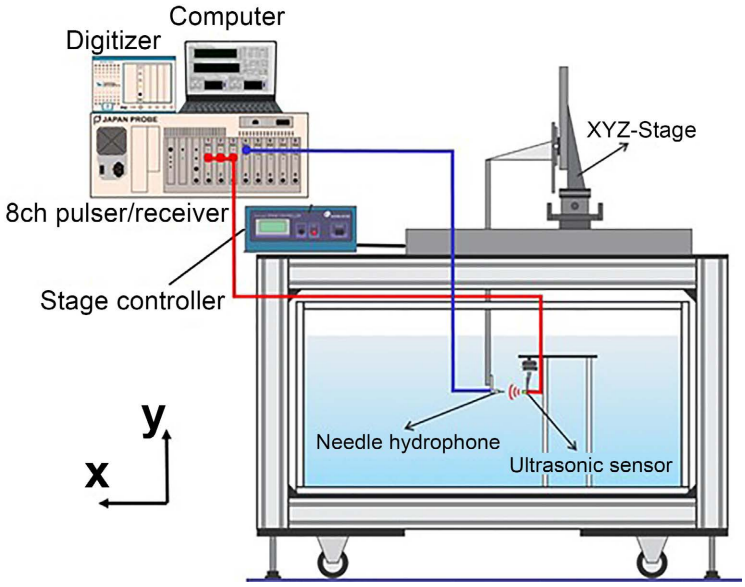

Figure 10. Experimental apparatus of the sound pressure measurement.

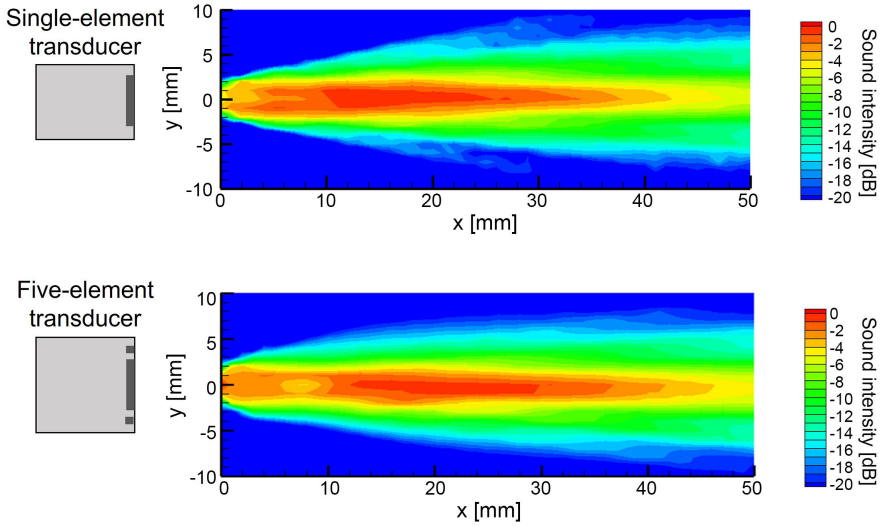

Figure 11. Result of the sound intensity measurement, (a) five-element transducer, (b) single element transducer.

with an active diameter of 5 mm. They had a good agreement with each other. The sound pressure transmitted in the axial distance (x) from transducer surface up to around 8 mm, the sound pressure showed fluctuation of sound intensity. In this region, the measurement volume is suspected to be not focused on the center, and several peaks are observed. It is called the near field region. Hence, multi-dimensional velocity measurement might not have the ability in the region with multi-peaks of intensity.

The sound distribution measured at the center of lateral distance and axial distance from 8 mm to 50 mm, on the other hand, had intensity more than −6 dB, which is a violent sound intensity. On the sound field, there was strong directivity and a narrow beam width of roughly 5 mm. This zone's sound field is

suitable for determining the velocity profile. As a result, the five-element transducer's ability to get multi-dimensional velocity per the research aim has been proven.

4. Accuracy Validation in Two-Dimensional Measurement

The experimental measurement in a rigid rotating cylinder was used to validate the accuracy of the UVP with a transducer constructed to acquire the multi-dimensional velocity. The measurement in two-dimensional (2D) was focused. The accuracy of the UVP was verified by comparing it with theoretical data. Figure 12 shows the experimental apparatus. The rectangular tank was filled with tap water that its temperature was kept at ≈26˚C ± 2˚C. The rotating cylinder contained tap water dispersed with nylon particle 80 μm, and its concentration was 1 g/litter. The cylinder was made from acrylic. The wall thickness was 3 mm. It was put on the rotating support. The motor rotates the cylinder. The rotating speed was set at 30 rpm. The five-element transducer was immersed in the water. The UVP measurement system employed has the same specification as section 3. The UVP parameter was set as shown in Table 2.

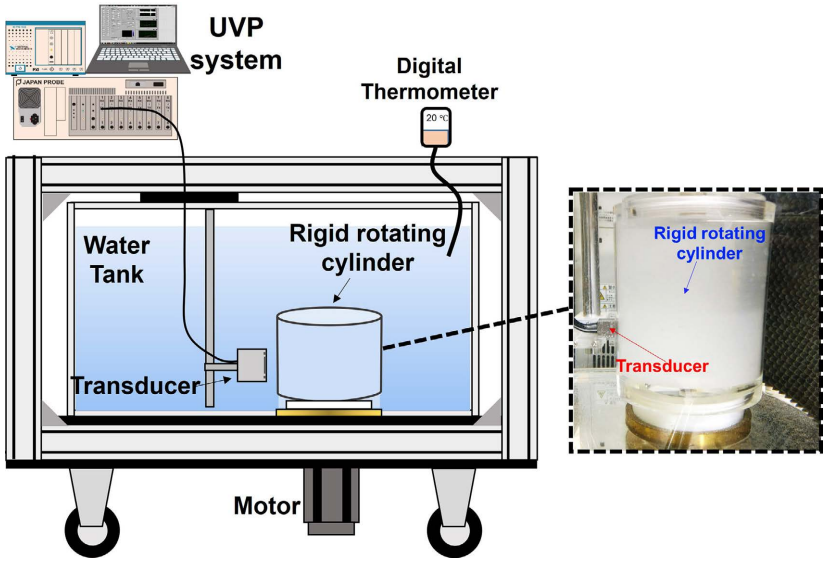

Figure 12. Experimental apparatus of the rigid rotating cylinder.

Table 2. Parameter setting of UVP system.

Condition	Detail
Basic frquency	4 MHz
Pulse repetition frequency	1 kHz
Number of cycles	4
Spatial resolution	0.74 mm
Number of repetition	128
Number of profiles	2000

Figure 13 shows the result of time-averaged axial and tangential velocity before reconstructing the 2D velocity profile. The result was validated with theoretical data. The theoretical velocity data can be derived using the equations below.

$$V_{x,theo}(i) = d_y(i)\omega_c$$
$$V_{y,theo}(i) = d_x(i)\omega_c \quad (17)$$

$V_{x,theo}$ and $V_{y,theo}$ are theoretical velocity components at each position, respectively. d_x and d_y are x and y-direction distance components from the center of the rotating cylinder, and ω_c is the rotating speed. There is good agreement between experiment and theoretical results in the axial velocity measuring distance of 15 mm to 150 mm. The measurement deviation enhanced continuously as increasing of measurement depth in the axial velocity profile. The factor of increasing deviation with the measurement depth is an ultrasonic attenuation during the propagation, and the signal to noise ratio of the echo signal is decreased. In addition, the ultrasonic pulse was transmitted from curved cylinder wall, then the ultrasonic path was refracted, and the measurement position was expected to different with assumed position; it's induced the absolute measurement error. Furthermore, the geometrically determined echo angles are employed to estimate the measurement velocity; however, as the measurement distance increases, the influence of the angle deviation on the measurement velocity increases. The theoretical value and the tangential velocity obtained from the measurement were identical. The standard deviation of the measurement was almost constant between 15 mm and 150 mm of the measurement distance because the influence of the echo angle deviation was smaller than the axial velocity. Both velocities derived from the measurement at the near-wall region were inaccurate and high discrepancy with the theoretical data. This was caused by near-field behavior and ultrasonic multi-reflection in the wall.

Figure 14 shows the 2D velocity profile reconstructed from the UVP measurement and theoretical calculation. The good agreement of both data were seen obviously with the discrepancy of velocity magnitude between them ±15%, as shown in Figure 15. The data out of the ±15% range are observed near the wall of the transducer, which is approximately 5 to 15 mm. Because of the near-field sound of the ultrasonic beam in this region, the sound pressure distribution is expected to be complicated, and the signal quality is lower. In addition, in this region, the echo signals reflected from the surface and inside the pipe wall overlap with the echo signals from the tracer particles in the fluid. Since the signals from the pipe wall are not accompanied by Doppler phase shift, the velocity near the pipe wall where these signals overlap is expected to be underestimated. It can be improved by performing a velocity correction that considers the measurement volume and position [29].

Therefore, it can be concluded that the measurement of this developed technique is feasible to obtain the multi-dimensional velocity profile.

5. Three-Dimensional Measurement in Turbulent and Swirling Pipe Flow

The ability of the UVP with the five-element transducer to measure the 3D velocity profile was demonstrated in this section. The experiment was conducted in the horizontal acrylic pipe (inner diameter, D: 50 mm) without and with a

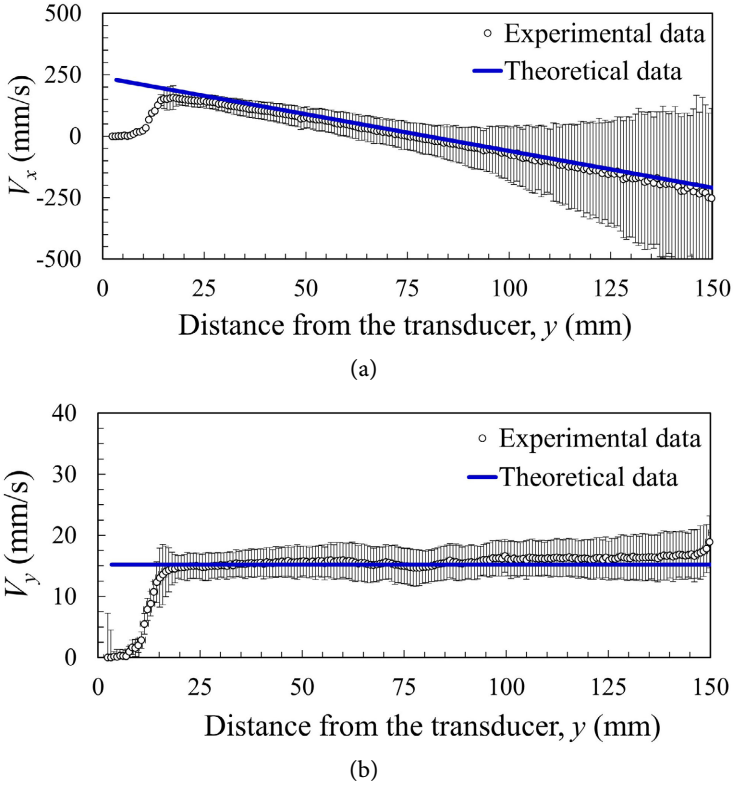

Figure 13. Result of the time-averaged velocity profiles in the rotating cylinder. (a) Axial velocity; (b) Tangential velocity.

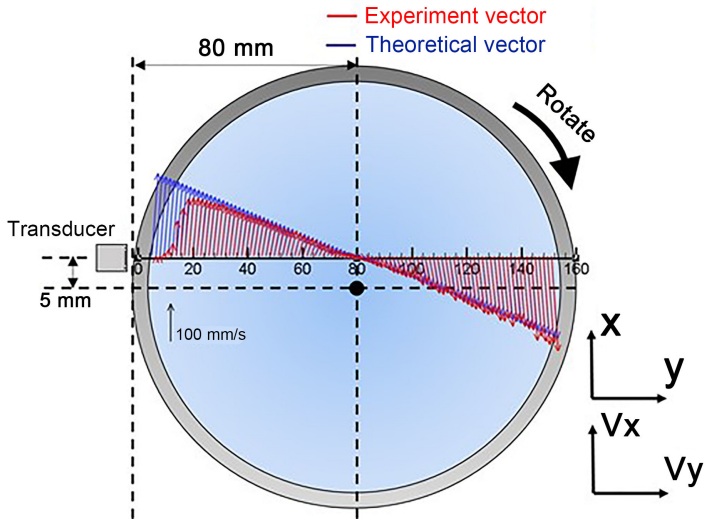

Figure 14. Result of the two-dimensional velocity vector profile in the rotating cylinder.

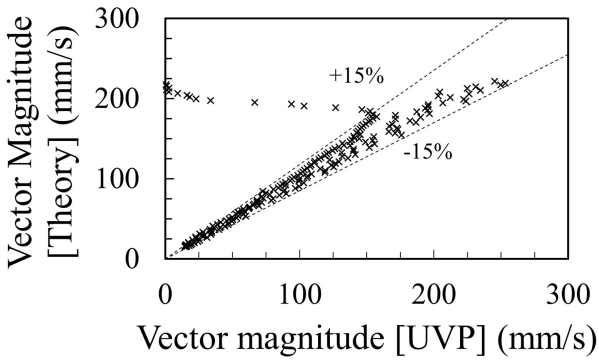

Figure 15. The discrepancy of the comparison between UVP and theoretical data.

swirling effect using a swirling generator (rotating pipe driven by a motor), as shown in **Figure 16**. The swirling generator consists of a 150 mm long aluminum pipe with an inner diameter of 50 mm. The small tubes of diameter 3 mm and 50 mm long are inserted into the aluminum pipe. The small tubes are packed as tightly as possible, and their number is approximately 95. The working fluid was tap water, with the temperature controlled by the cooling system. The water temperature was set at 25˚C. Nylon particle with a diameter of 80 μm was dispersed in the water used as a liquid tracer, and its concentration was 1 g/litter. The liquid flow rate was controlled by the ball valve and was measured by an electromagnetic flow meter. The transducer was installed at the test section, placed at 43D from the flow conditioner, and immersed in water as a coupling fluid. In the swirling case, the swirling generator was installed in 3D from the test section. The UVP system employed consisted of the five-element transducer, which was connected to the 8 ch pulser/receiver. Echo output from pulse/receiver was sent to the A/D converter. This equipment was connected to a PC and controlled by a developed UVP program made in LabVIEW 2011. All UVP equipment was similar to chapter 4. The experimental condition and measurement parameters setting are presented in **Table 3** and **Table 4**. Firstly, the experimental measurement was conducted in a turbulent flow condition. After that, the experiment was executed in swirling flow conditions. The 2D velocity profile in an axial and radial plane was derived. Then, the 3D velocity profile was reconstructed.

Figure 17 represents the measurement result in a turbulent flow. The velocity profile in axial (V_x), tangential (V_y), and radial (V_z) directions were derived simultaneously. The error bars represent the standard deviation. The profile near the wall region (approximately 0 to 5 mm) indicated a high fluctuation. The region has high turbulence intensity in the pipe since the region is the viscous sublayer to the transition layer. In addition, because of the near-field region of the ultrasonic beam, the sound pressure distribution formed is expected to be complex. Therefore, it is thought that the high fluctuation near the wall was due to the high-velocity fluctuation of the fluid itself and the low signal quality caused by the characteristics of the ultrasonic beam. The profile apart from the

near field region can be obtained. The velocity level in the axial axis at the center of the pipe was 330 mm/s. The velocity at the wall region was approximately 200 mm/s. The tangential and radial velocity was approximately near zero due to the flow is fully developed. The accuracy of axial velocity was confirmed by comparing the velocity profile with the profile derived from the single ultrasonic transducer and power-law of velocity distribution, as illustrated in Figure 18. The power-law velocity profile can be derived as the following equation using a flow rate in a pipe, Q, and inner pipe diameter, D, below.

Table 3. Experimental condition.

Condition	Detail
Reynolds number	15,000
Pipe inner diameter (D)	50 mm
Water tmperature	25˚C ± 2˚C
Motor frequency (in swiring case)	600 rpm
Swiring intensity (in swiring case)	0.5

Table 4. Parameter setting of UVP system.

Condition	Detail
Basic frquency	4 MHz
Pulse repetition frequency	1 kHz
Number of cycles	4
Spatial resolution	0.74 mm
Number of repetition	128
Number of profiles	5000

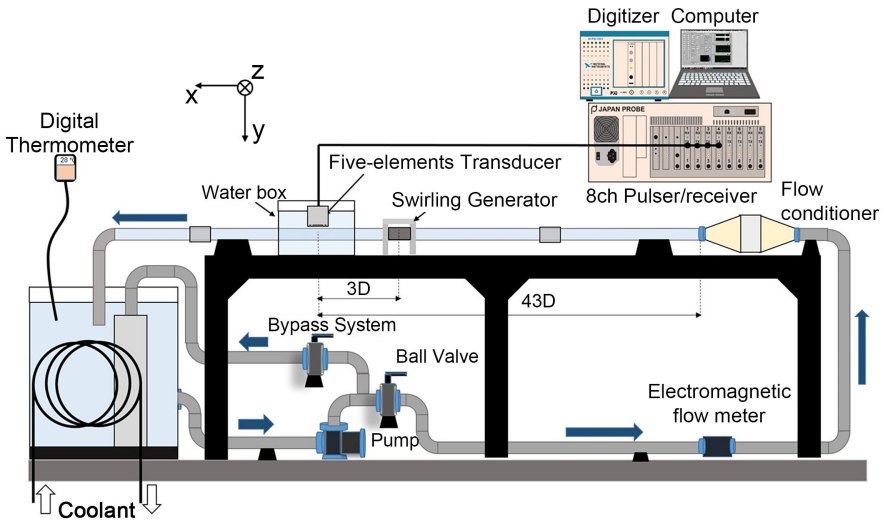

Figure 16. Experimental apparatus of the horizontal pipe flow measurement.

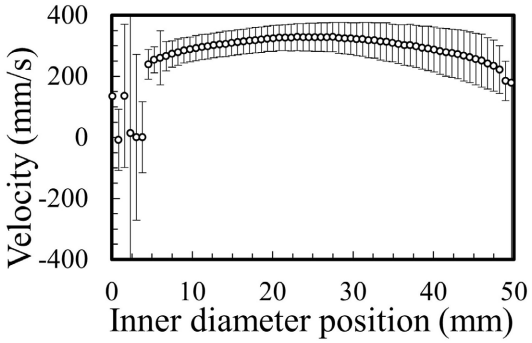

(a)

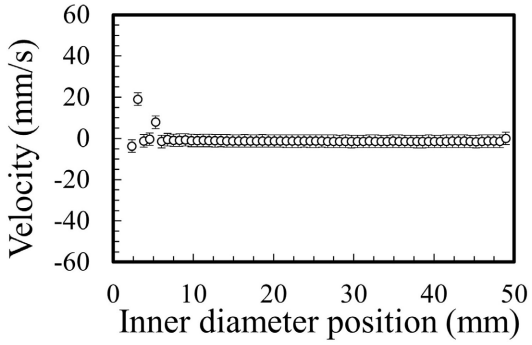

(b)

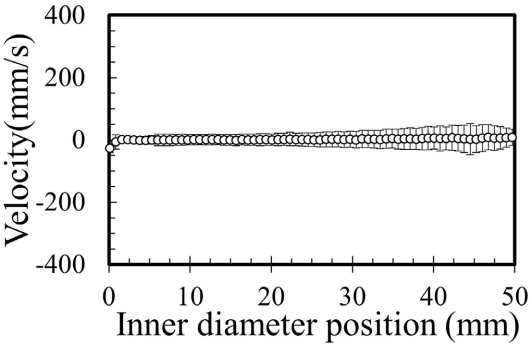

(c)

Figure 17. Three-dimensional velocity profile of fully developed turbulent flow, (a) Axial velcoity, (b) Tangential velocity, (c) Radial velocity.

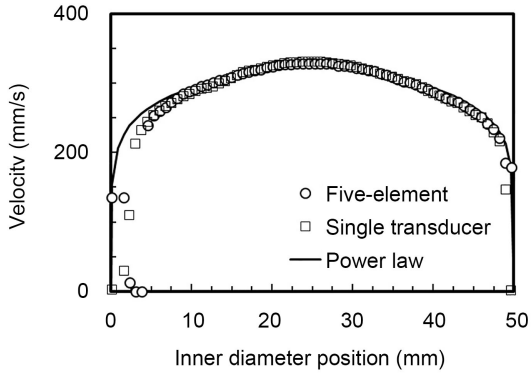

(a)

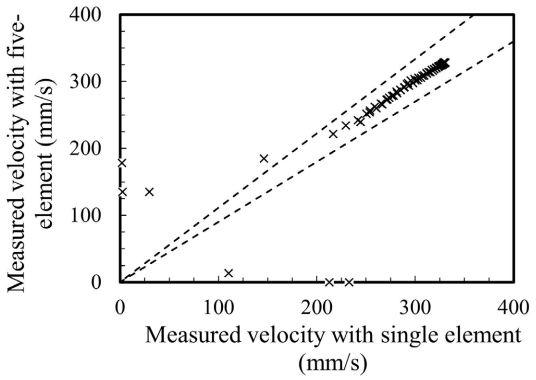

(b)

Figure 18. The comparison result of the axial velocity between five-element transducer and single element transducer, (a) velocity profile, (b) discrepancy.

$$u(y)=\frac{(n+1)(2n+1)}{2n^2}\frac{4Q}{\pi D^2}\left(\frac{2y}{D}\right)^{\frac{1}{n}}, \tag{18}$$

where y is the distance from the pipe wall, in the fully developed turbulent flow, a constant value, n depends on the Reynolds number, Re. The Reynolds number of this experiment was 1.5×10^4, and the index, n, was determined as 7. In comparison with the power-law velocity profile, good agreement was observed in the main flow area near the center of the pipe. In contrast, near the pipe wall, the measurement results by the five-element transducer were lower than the power law. The measured velocity is an average value in the measurement volume and is underestimated in the high-velocity gradient region. This is also the case for the conventional single transducer measurement, a common problem for UVP. To improve the problem, it is necessary to use smaller wavelengths (higher ultrasonic fundamental frequencies) to reduce the measurement volume. The discrepancy of the validation between five-element and single-element transducer was within ±10%. **Figure 19(a)** and **Figure 19(b)** illustrate the 2D velocity profile in the axial plane (x-y) and radial plane (z-y) reconstructed. The velocity vector in the axial plane was mostly in the horizontal direction. Its magnitude was similar to the axial velocity presented in **Figure 17(a)**, owing to very small motion in a tangential and radial direction. Hence, the vector magnitude in the radial plane observed is very small. Then, the 3D velocity profile was reconstructed, as shown in **Figure 19(c)**.

Next, the ability of the UVP with the five-element transducer in 3D measurement was demonstrated by experimenting with swirling flow. In this experiment, the swirling intensity S that can be defined as the ratio of the circumferential momentum and the axial momentum was set to 0.5. The swirling intensity S is derived by the following equation: the angular velocity ω of the rotary pipe, pipe diameter D, and bulk velocity U_m of the flow [30].

$$S=\frac{\omega D}{2U_m}. \tag{19}$$

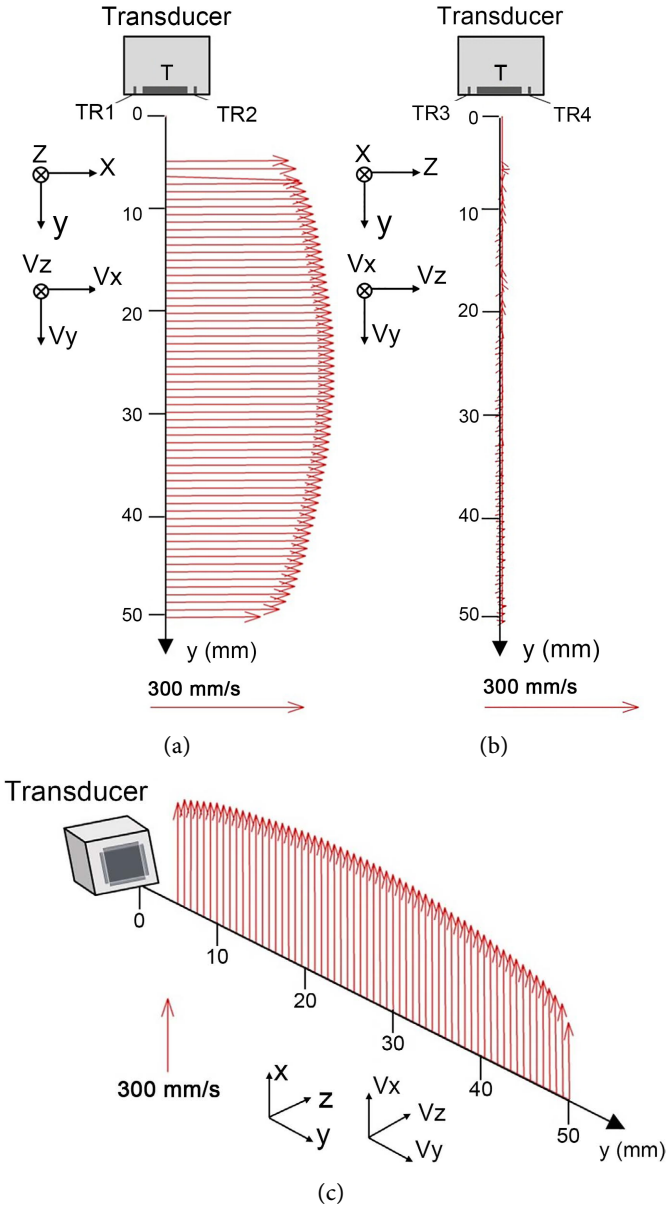

Figure 19. Three-dimensional velcoity vector profile of fully developed turbulent flow, (a) 2D velocity in the axial plane, (b) 2D velocity in the radial plane, (c) 3D velocity profile.

The pipe can be rotated about its axis at speed varying from 15 to 1100 rpm by an induction motor (5IK90SW-5 Oriental Motor Co., Ltd.), and a timing belt. With the pipe rotation, the growth of the boundary layer on the pipe walls establishes an azimuthal velocity distribution corresponding to the solid-body rotation in the core. The rotary swirling allows the solid rotation of the small tubes in the peripheral direction, while the function generates the uniform axial velocity distribution [31]. **Figure 20** represents the measurement result in swirling flow. The velocity profile in the axial (*x*-*y*) and radial (*z*-*y*) planes was obtained simultaneously. The profile in the near field zone was still unable to be measured. The profile beyond the near field region can be obtained. The 2D velocity profile

in the axial plane (*x*-*y*) was mostly in the horizontal direction. Non fully developed flow motion was seen, obviously. In a radial plane, a swirling motion of the 2D flow field was observed. Then, the 3D velocity profile in the swirling flow was reconstructed, as shown in Figure 20(c).

The three-dimensional motion of this flow was observed. Therefore, it can be summarized that the UVP collaborated with compact transducer has applicability to obtain the multi-dimensional velocity profile and fulfill the demand of visualization in fluid engineering.

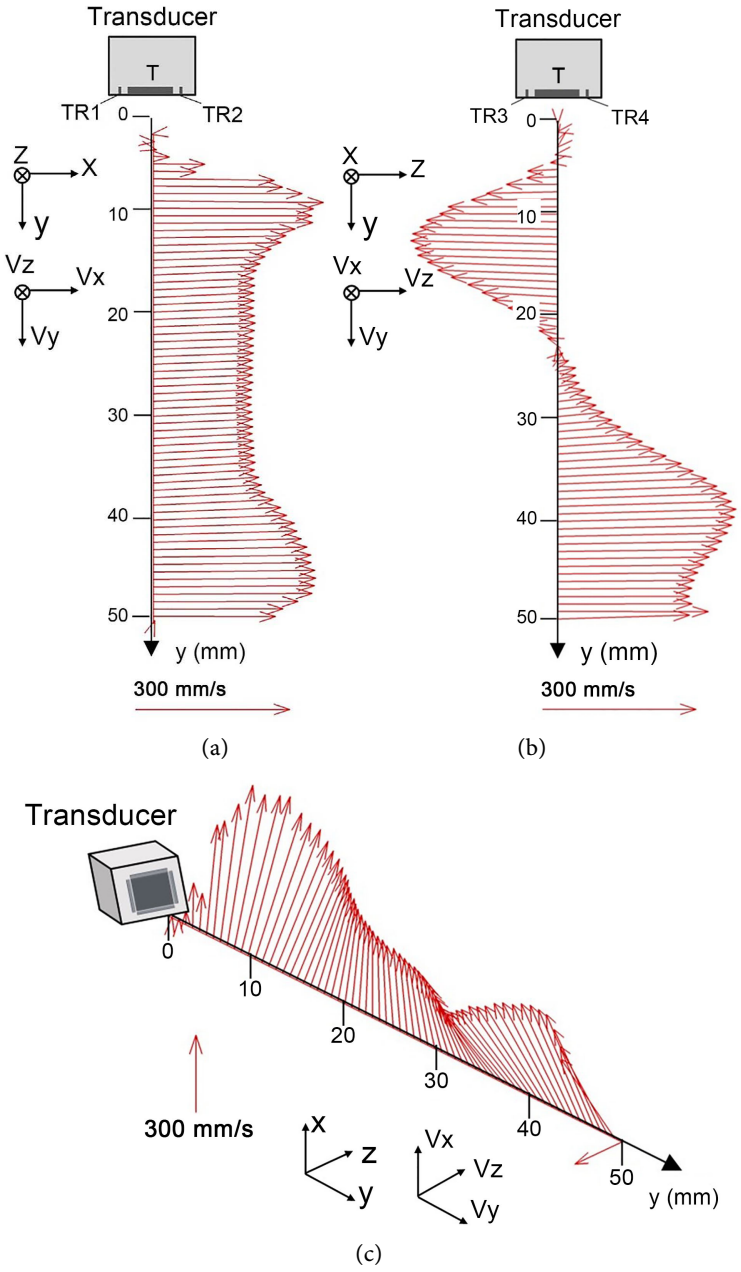

Figure 20. Three-dimensional velocity vector profile of swirling flow, (a) 2D velocity in the axial plane, (b) 2D velocity in the radial plane, (c) 3D velocity profile.

6. Conclusions

The ultrasonic velocity profiler with a new ultrasonic array transducer with a special configuration of five elements was developed. One element works as a transmitter and four elements as a receiver. The four receivers received four Doppler frequencies. Three-dimensional velocity information along the measurement line can be reconstructed.

The basic frequency was selected to be compatible with the application. The sound intensity distribution of the manufactured transducer was evaluated and proved.

The measurement ability of the UVP with a five-element transducer was demonstrated. The measurement accuracy in two-dimensional flow was evaluated by comparing it with the theoretical data. The uncertainty of the validation was inside 15%. Then, the three-dimensional measurement in turbulent flow was demonstrated experimentally. The 2D velocity profile was obtained. The axial velocity received by the five-element transducer has a good agreement with the single element transducer as the measurement comparison. Finally, measurements were conducted on the swirling flow. The three-dimensional velocity with swirling motion was observed. This reflects the ability of the developed system the measurement of the velocity profile in multi-dimensional motion.

The measurement accuracy of this method is mainly determined by the basic ultrasonic frequency and the uncertainty of the echo angle. An element with a higher basic frequency can achieve a smaller measurement volume and higher velocity resolution. However, a higher frequency causes a lower measurable distance due to higher attenuation. Therefore, it is a trade-off between the desired accuracy and the measurement distance. It needs to determine the transducer parameters according to the application.

Conflicts of Interest

The authors declare no conflicts of interest regarding the publication of this paper.

References

[1] Chang, D. and Tavoularis, S. (2015) Hybrid Simulations of the Near Field of a Split-Vane Spacer Grid in a Rod Bundle. *International Journal of Heat and Fluid Flow*, **51**, 151-165. https://doi.org/10.1016/j.ijheatfluidflow.2014.07.005

[2] Li, H. and Tomita, Y. (2000) Particle Velocity and Concentration Characteristics in a Horizontal Dilute Swirling Flow Pneumatic Conveying. *Powder Technology*, **107**, 144-152. https://doi.org/10.1016/S0032-5910(99)00181-3

[3] Sommerfeld, M. and Qiu, H.H. (1991) Detailed Measurements in a Swirling Particulate Two-Phase Flow by a Phase-Doppler Anemometer. *International Journal of Heat and Fluid Flow*, **12**, 20-28. https://doi.org/10.1016/0142-727X(91)90004-F

[4] Rehme, K. (1987) The Structure of Turbulent Flow through Rod Bundles. *Nuclear Engineering and Design*, **99**, 141-154.

https://doi.org/10.1016/0029-5493(87)90116-6

[5] Neti, S., Eichhorn, R. and Hahn, O.J. (1983) Laser Doppler Measurements of Flow in a Rod Bundle. *Nuclear Engineering and Design*, **74**, 105-116. https://doi.org/10.1016/0029-5493(83)90143-7

[6] Ikeda, K. and Hoshi, M. (2006) Development of Rod-Embedded Fiber LDV to Measure Velocity in Fuel Rod Bundles. *Journal of Nuclear Science and Technology*, **43**, 150-158. https://doi.org/10.1080/18811248.2006.9711077

[7] Kumar, R. and Conover, T. (1993) Flow Visualization Studies of a Swirling Flow in a Cylinder. *Experimental Thermal and Fluid Science*, **7**, 254-262. https://doi.org/10.1016/0894-1777(93)90009-8

[8] McClusky, H.L., Holloway, M.V., Beasley, D.E. and Conner, M.E. (2002) Development of Swirling Flow in a Rod Bundle Subchannel. *Journal of Fluids Engineering*, **124**, 747-755. https://doi.org/10.1115/1.1478066

[9] Satomura, S. (1957) Ultrasonic Doppler Method for the Inspection of Cardiac fuNctions. *The Journal of the Acoustical Society of America*, **29**, 1181-1185. https://doi.org/10.1121/1.1908737

[10] Baker, D.W. (1970) Pulsed Ultrasonic Doppler Blood-Flow Sensing. *IEEE Transactions on Sonics and Ultrasonics*, **17**, 170-185. https://doi.org/10.1109/T-SU.1970.29558

[11] Peronneau, P., Sandman, W. and Xhaard, M. (1977) Blood Flow Patterns in Large Arteries. In: White, D.N. and Brown, R.E., Eds., *Ultrasound in Medicine*, Vol. 3B, Plenum Press, New York, London, 1193-1208.

[12] Scabia, M., Calzolai, M., Capineri, L., Masotti, L. and Fort, A. (2000) A Real-Time Two-Dimensional Pulsed-Wave Doppler System. *Ultrasound in Medicine and Biology*, **26**, 121-131. https://doi.org/10.1016/S0301-5629(99)00115-5

[13] Fox, M.D. and Gardiner, M.W. (1988) Three-Dimensional Doppler Velocimetry of Flow Jets. *IEEE Transactions on Biomedical Engineering*, **35**, 834-841. https://doi.org/10.1109/10.7290

[14] Dunmire, B.L., Beach, K.W., Labs, K.H., Detmer, P.R. and Strandness, D.E. (1995) A Vector Doppler Ultrasound Instrument. *Proceedings of the* 1995 *IEEE Ultrasonics Symposium*, Vol. 2, Seattle, 7-10 November 1995, 1477-1480. https://doi.org/10.1109/ULTSYM.1995.495834

[15] Takeda, Y. (1986) Velocity Profile Measurement by Ultrasonic Doppler Shift Method. *International Journal of Heat and Fluid Flow*, **7**, 313-318. https://doi.org/10.1016/0142-727X(86)90011-1

[16] Takeda, Y. (1991) Development of an Ultrasound Velocity Profile Monitor. *Nuclear Engineering and Design*, **126**, 277-284. https://doi.org/10.1016/0029-5493(91)90117-Z

[17] Kikuchi, K., Takeda, Y., Obayashi, H., Tezuka, M. and Sato, H. (2006) Measurement of LBE Flow Velocity Profile by UDVP. *Journal of Nuclear Materials*, **356**, 273-279. https://doi.org/10.1016/j.jnucmat.2006.05.028

[18] Kikura, H., Takeda, Y. and Durst, F. (1999) Velocity Profile Measurement of the Taylor Vortex Flow of a Magnetic Fluid Using the Ultrasonic Doppler Method. *Experiments in Fluids*, **26**, 208-214. https://doi.org/10.1007/s003480050281

[19] Eckert, S. and Gerbeth, G. (2002) Velocity Measurements in Liquid Sodium by Means of Ultrasound Doppler Velocimetry. *Experiments in Fluids*, **32**, 542-546. https://doi.org/10.1007/s00348-001-0380-9

[20] Mori, M., Takeda, Y., Taishi, T., Furuichi, N., Aritomi, M. and Kikura, H. (2002)

Development of a Novel Flow Metering System Using Ultrasonic Velocity Profile Measurement. *Experiments in Fluids*, **32**, 153-160. https://doi.org/10.1007/s003480100295

[21] Kikura, H., Yamanaka, G. and Aritomi, M. (2004) Effect of Measurement Volume Size on Turbulent Flow Measurement Using Ultrasonic Doppler Method. *Experiments in Fluids*, **36**, 187-196. https://doi.org/10.1007/s00348-003-0694-x

[22] Batsaikhan, M., Zhang, Z.L., Takahashi, H. and Kikura, H. (2021) Development of Measurement System for Flow and Shape Using Array Ultrasonic Sensors. *Journal of Flow Control, Measurement & Visualization*, **9**, 45-72. https://doi.org/10.4236/jfcmv.2021.93004

[23] Hamdani, A., Ihara, T. and Kikura, H. (2016) Experimental and Numerical Visualization of Swirling Flow in a Vertical Pipe. *Journal of Visualization*, **19**, 369-382. https://doi.org/10.1007/s12650-015-0340-8

[24] Shwin, S., Hamdani, A., Takahashi, H. and Kikura, H. (2017) Experimental Investigation of Two-Dimensional Velocity on the 90° Double Bend Pipe Flow Using Ultrasound Technique. *World Journal of Mechanics*, **7**, 340-359. https://doi.org/10.4236/wjm.2017.712026

[25] Takahashi, H., Shwin, S., Hamdani, A., Fujisawa, N. and Kikura, H. (2020) Experimental and Numerical Investigation of Swirling Flow on Triple Elbow Pipe Layout. *Journal of Flow Control, Measurement & Visualization*, **8**, 45-62. https://doi.org/10.4236/jfcmv.2020.82003

[26] Hurther, D. and Lemmin, U. (1998) A Constant-Beam-Width Transducer for 3D Acoustic Doppler Profile Measurements in Open-Channel Flows. *Measurement Science and Technology*, **9**, 1706-1714. https://doi.org/10.1088/0957-0233/9/10/010

[27] Kasai, C., Namekawa, K., Koyano, A. and Omoto, R. (1985) Real-Time Two Dimensional Blood Flow Imaging Using an Autocorrelation Technique. *IEEE Transactions on Sonic and Ultrasonic*, **32**, 458-464. https://doi.org/10.1109/T-SU.1985.31615

[28] Banerjee, S., Kundu, T. and Placko, D. (2006) Ultrasonic Field Modeling in Multilayered Fluid Structures Using the Distributed Point Source Method Technique. *Journal of Applied Mechanics*, **73**, 598-609. https://doi.org/10.1115/1.2164516

[29] Taishi, T., Kikura, H. and Aritomi, M. (2002) Effect of the Measurement Volume in Turbulent Pipe Flow Measurement by the Ultrasonic Velocity Profile Method (Mean Velocity Profile and Reynolds Stress Measurement). *Experiments in Fluids*, **32**, 188-196. https://doi.org/10.1007/s003480100299

[30] Rocklage-Marliani, G., Schmidts, M. and Ram, V.I.V. (2003) Three-Dimensional laser-Doppler Velocimeter Measurements in Swirling Turbulent Pipe Flow. *Flow, Turbulence and Combustion*, **70**, 43-67. https://doi.org/10.1023/B:APPL.0000004913.82057.81

[31] Takano, T., Ikarashi, Y., Uchiyama, K., Yamagata, T. and Fujisawa, N. (2016) Influence of Swirling Flow on Mass and Momentum Transfer Downstream of a Pipe with Elbow and Orifice. *International Journal of Heat and Mass Transfer*, **92**, 394-402. https://doi.org/10.1016/j.ijheatmasstransfer.2015.08.087

Nomenclature

a: Transmitter element width [m]
b: Receiver element width [m]
c: Sound speed [m/s]
d_x: X component of distance from the rotating cylinder center [m]
d_y: Y component of distance from the rotating cylinder center [m]
D: Inner pipe diameter [m]
e: Echo signal
f_0: Ultrasonic basic frequency [Hz]
f_d: Doppler frequency [Hz]
f_{PRF}: Pulse repetition frequency [Hz]
g: Transmitter-receiver gap [m]
h_I: In-phase component of demodulated signal
h_Q: Quadrature-phase component of demodulated signal
i: Measurement position
l: Element length [m]
n: Index of pulse repetition
R_A: Real component of autocorrelation function
R_B: Imaginary component of autocorrelation function
Re: Reynolds number [-]
R_m: Autocorrelation function
S: Swirling intensity [-]
SI: Sound intensity [dB]
t: Delay time of echo signal
U_m: Bulk velocity [m/s]
V: Velocity [m/s]
V_{axial}: Axial velocity [m/s]
V_{radial}: Radial velocity [m/s]
V_x: X component velocity [m/s]
$V_{x,theo}$: Theoretical x component velocity [m/s]
V_y: Y component velocity [m/s]
$V_{y,theo}$: Theoretical y component velocity [m/s]
V_z: Z component velocity [m/s]
x: Distance of x direction [m]
y: Distance of y direction [m]
z: Distance of z direction [m]
θ: Echo angle [rad]
λ: Wavelength [m]
τ: Traveling time of ultrasound [s]
φ: Initial phase of echo signal [rad]
ω: Angular velocity of swirling generator [rad/s]
ω_c: Angular velocity of rotating cylinder [rad/s]